Stochastic chaos and resonance in a bistable stochastic system

Sukkeun Kim and L. E. Reichl
Center for Studies in Statistical Mechanics and Complex Systems, The University of Texas at Austin, Austin, Texas 78712
(Received 31 August 1995; revised manuscript received 29 November 1995)

We study a periodically driven bistable system in the presence of fluctuations. The spectral properties of the Fokker-Planck equation are studied using the finite element method. The ground Floquet state exhibits stochastic resonance. The dynamics of the Fokker-Planck equation governing the system is equivalent to that of a quantum system governed by an underlying Hamiltonian that can be obtained from the Fokker-Planck equation. When the Hamiltonian system exhibits the transition to chaos, the decay rates of the Fokker-Planck equation show level repulsion.

PACS number(s): 05.40.+j, 02.50.−r, 05.45.+b

I. INTRODUCTION

The transition to chaos in a classical system has been found to manifest itself in its quantum counterpart in several ways [1]. One commonly observed manifestation is the onset of level repulsion in the nearest neighbor energy level spacing distribution of a quantum system as its classical counterpart undergoes a transition to chaos. Recently, Millonas and Reichl [2] have shown that a large class of Fokker-Planck equations, which describe Brownian motion in two spatial dimensions, can exhibit a transition in their spectral statistics as a coupling parameter is varied. They showed that the dynamics of the Fokker-Planck equation governing the system is equivalent to that of a quantum system governed by a Hamiltonian that can be obtained from the Fokker-Planck equation through an appropriate transformation. When the Hamiltonian system exhibits the transition to chaos, the decay rates of the Fokker-Planck equation show level repulsion. A similar phenomenon was observed by Alpatov and Reichl [3] for a one-dimensional Brownian rotor driven by a time-periodic force. They found that the behavior of the Fokker-Planck equation could be related to a time-periodic Hamiltonian. As that Hamiltonian underwent a transition to chaos the decay rates exhibited level repulsion and dramatically decreased the time necessary for the system to reach its long-time state.

In this paper, we consider a system that has been studied by many authors because of its wide range of applications, but we analyze it in a completely different way. We consider a Brownian particle moving in a quartic potential well and driven by a time-periodic force. For the case when the friction acting on the Brownian particle is very strong (the overdamped case), the Brownian particle obeys the Langevin equation

$$\frac{dx}{dt}=x-x^3+\epsilon\,\sin(\Omega t)+\xi(t), \tag{1}$$

where ϵ is the strength and Ω is the frequency of the periodic driving force, and $\xi(t)$ is a random force which has zero mean and is δ correlated,

$$\langle\xi(t)\rangle=0 \quad \text{and} \quad \langle\xi(t')\xi(t)\rangle=g\,\delta(t'-t). \tag{2}$$

In Eq. (2), g is the diffusion coefficient and is a measure of the strength of the random force. This system has been studied in several different contexts. For example, Eq. (1) is closely related to an approximate equation, obtained from the stochastic Swift-Hohenberg equation, which describes the time evolution of the amplitude of a single convection mode in a finite Rayleigh-Bernard system [4,5]. Also, it has been used as a paradigm model to describe the phenomenon of *stochastic resonance* [6–14] and some general features of the long-time state [15]. Stochastic resonance is a property of the long-time state of this system. While we consider stochastic resonance in this paper, our focus will be on the effect of an underlying transition to chaos on the rate of approach to the long-time state.

In Sec. II we write down the Fokker-Planck equation and describe how to use Floquet theory to obtain the Floquet decay rates. In Sec. III we obtain a Schrödinger-like equation from the Fokker-Planck equation through an appropriate transformation. In Sec. IV we examine the Hamiltonian dynamics underlying this system and the effect on the spectrum of decay rates of the transition to chaos. In Sec. V, we show the regime of stochastic resonance, and finally in Sec. VI we make some concluding remarks.

II. THE FOKKER-PLANCK EQUATION

Let us consider a Brownian particle moving in a double well potential, $U(x)=-\frac{1}{2}x^2+\frac{1}{4}x^4$, and driven by a time-period force, $F(t)=\epsilon\,\sin(\Omega t)$. The Langevin equation, for large friction, is given by

$$\frac{dx}{dt}=-U_x(x)+F(t)+\xi(t), \tag{3}$$

where $U_x(x)=dU(x)/dx$ and $\xi(t)$ is defined in Eq. (2). The Fokker-Planck equation corresponding to the Langevin equation is

$$\frac{\partial P(x,t)}{\partial t}=\frac{\partial}{\partial x}\{[U_x(x)-F(t)]P(x,t)\}+\frac{g}{2}\frac{\partial^2 P(x,t)}{\partial x^2}$$
$$\equiv\hat{L}_{FP}(x,t)P(x,t), \tag{4}$$

where $P(x,t)$ is the probability to find the Brownian particle in the interval $x \rightarrow x+dx$ at time t, and $\hat{L}_{FP}(x,t)$ is the Fokker-Planck operator for this system,

$$\hat{L}_{FP}(x,t)=U_{xx}(x)+[U_x(x)-F(t)]\frac{\partial}{\partial x}+\frac{g}{2}\frac{\partial^2}{\partial x^2}. \quad (5)$$

The equation (4) has a time-periodic drift coefficient with period, $T=2\pi/\Omega$. Therefore, it has the Floquet-type solutions

$$P_\alpha(x,t)=e^{-\lambda_\alpha t}\Phi_\alpha(x,t), \quad (6)$$

where λ_α is the αth Floquet decay rate and $\Phi_\alpha(x,t)$ is the αth Floquet eigenstate and is time-periodic with period, T. That is, $\Phi_\alpha(x,t)=\Phi_\alpha(x,t+T)$. The decay rates, λ_α, are, in general, complex, since the Fokker-Planck operator, $\hat{L}_{FP}(x,t)$, is non-self-adjoint. The probability density, $P(x,t)$, is a conserved quantity, so the real part of λ_α must be non-negative.

The Floquet eigenvalue equation takes the form

$$\left(\frac{\partial}{\partial t}-\hat{L}_{FP}(x,t)\right)\Phi_\alpha(x,t)=\lambda_\alpha\Phi_\alpha(x,t). \quad (7)$$

Since $\Phi_\alpha(x,t)$ is time periodic, we can expand the time dependent part in a Fourier series and the space dependent part in terms of a complete set of orthogonal functions, $\phi_n(x)$, on interval $-\infty \leq x \leq \infty$. Thus we can write

$$\Phi_\alpha(x,t)=\sum_{n=-\infty}^{\infty}\sum_{p=-\infty}^{\infty}a_\alpha(n,p)\phi_n(x)e^{ip\Omega t}. \quad (8)$$

We have used a finite element method to solve the eigenvalue equation, (7). This method is described in Appendix A. The Floquet matrix block diagonalizes due to the invariance of the Fokker-Planck operator under the generalized parity transformation, $x \rightarrow -x$ and $t \rightarrow t+T/2$. Then Floquet eigenstates are either even or odd under this transformation. In Fig. 1 we show part of the spectrum of Floquet decay rates for diffusion coefficent, $g=0.02$, driving field frequency, $\Omega=0.1$, and for a range of external field amplitudes, $\epsilon=0.0$, 0.05, 0.1. The horizontal axis is the real part of λ and gives the decay rate for that state, and the vertical axis is the imaginary part of λ and gives an oscillatory contribution to the time evolution. The spectrum shown in Fig. 1 contains eigenvalues associated with one block of the Fokker-Planck operator. The other block looks the same except that the imaginary part is shifted by $i\Omega$. Alternate points along the line, $\mathrm{Re}(\lambda)=0$, are nearly degenerate. They contain two eigenvalues, one at $\mathrm{Re}(\lambda)=0$ and another with $\mathrm{Re}(\lambda)>0$ but very small. The third line (from the left) of eigenvalues is also nearly degenerate. The points cannot be resolved on the scale shown.

The probability, $P(x,t)$, may be expanded in terms of Floquet states,

$$P(x,t)=\sum_\alpha A_\alpha e^{-\lambda_\alpha t}\Phi_\alpha(x,t), \quad (9)$$

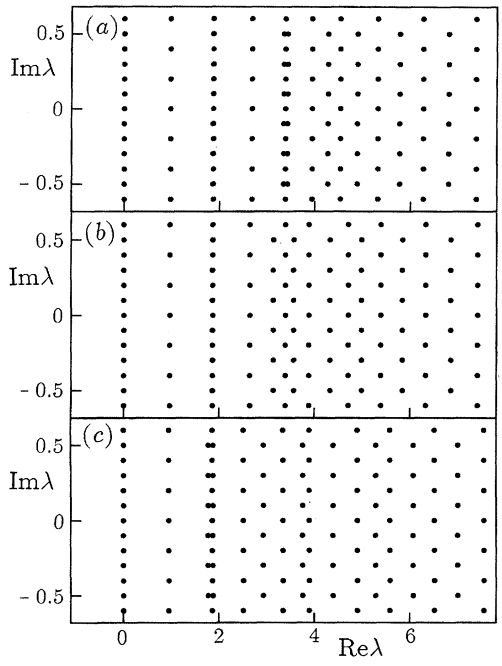

FIG. 1. Partial view of the spectrum of Floquet decay rates for $g=0.02$, $\Omega=0.1$, and (a) $\epsilon=0.0$, (b) $\epsilon=0.05$, (c) $\epsilon=0.1$. Only those Floquet decay rates in the neighborhood of $\lambda=0.0$ are shown.

where A_α is the weighting factor for the αth Floquet eigenstate. Notice that the spectrum forms a regular grid. The spacing between neighboring values, $\mathrm{Im}(\lambda_\alpha)$, is always a multiple of the driving field frequency, Ω. The fact that this must be so was proved in Ref. [3] and is a consequence of the time-periodicity of the Fokker-Planck operator. As we shall show in the next section, it is necessary to transform the Fokker-Planck equation in order to understand the structure of this Floquet spectrum.

III. SCHRÖDINGER-LIKE EQUATION

Let us now introduce the following transformation on the Fokker-Planck equation:

$$P(x,t)=e^{\{[-U(x)+xF(t)]/g\}}\Psi(x,t). \quad (10)$$

The function, $\Psi(x,t)$, then satisfies the Schrödinger-like equation

$$-g\frac{\partial\Psi(x,t)}{\partial t}=\hat{H}(x,t)\Psi(x,t), \quad (11)$$

where

$$\hat{H}(x,t)=\hat{H}_o(x)+\Delta\hat{V}_\epsilon(x,t) \quad (12)$$

is a self-adjoint time-periodic Hamiltonian-like operator. Equation (11) differs from a Schrödinger equation in that there is no factor of i in front of the time derivative. Therefore, the time evolution of the eigenstates is qualitatively different from that of a Schrödinger equation. The self-adjoint operator, $\hat{H}_o(x)$, is defined as

$$\hat{H}_o(x) = -\frac{g^2}{2}\frac{\partial^2}{\partial x^2} + V_o(x), \tag{13}$$

where

$$V_o(x) = -\frac{g}{2}U_{xx}(x) + \frac{1}{2}U_x^2(x)$$
$$= +\frac{g}{2} + \frac{1}{2}(1-3g)x^2 - x^4 + \frac{1}{2}x^6. \tag{14}$$

The time-periodic perturbation is given by

$$\Delta V_\epsilon(x,t) = -U_x(x)F(t) + \tfrac{1}{2}F^2(t) + x\frac{\partial F(t)}{\partial t}$$
$$= \epsilon(x - x^3)\sin(\Omega t) + \tfrac{1}{2}\epsilon^2 \sin^2(\Omega t)$$
$$+ \epsilon\Omega x \cos(\Omega t). \tag{15}$$

In the limit, $\epsilon \to 0$, the Hamiltonian dynamics is governed by the diffusion dependent potential, $V_0(x)$. We have now formulated this stochastic system in a form analogous to quantum mechanics if we let the diffusion coefficient play the role of Planck's constant. This transformation for the case $\epsilon = 0$ is described in Ref. [16].

The Schrödinger-like equation will also have Floquet solutions which we denote $\Psi_\alpha(x,t) = e^{-\lambda_\alpha t}\Pi_\alpha(x,t)$. The function, $\Pi_\alpha(x,t)$, is time periodic, $\Pi_\alpha(x,t) = \Pi_\alpha(x,t+T)$, and satisfies the eigenvalue equation,

$$g\lambda_\alpha \Pi_\alpha(x,t) = \left(\hat{H}(x,t) + g\frac{\partial}{\partial t}\right)\Pi_\alpha(x,t)$$
$$= \left(\hat{H}_0(x) + \Delta\hat{V}_\epsilon(x,t) + g\frac{\partial}{\partial t}\right)\Pi_\alpha(x,t). \tag{16}$$

The spectrum of decay rates, λ_α, is unchanged by this transformation. We could also obtain Eq. (16) by transforming directly the Floquet eigenfunctions. That is,

$$\Phi_\alpha(x,t) = e^{[-U(x)+xF(t)]/g}\Pi_\alpha(x,t). \tag{17}$$

The Floquet operator, $\hat{H}_F = \hat{H} + g\,\partial/\partial t$, is non-self-adjoint. The first thing to notice about Eq. (16) is that in the limit, $\epsilon \to 0$, $\lambda_\alpha \to E_n/g + ip\Omega$, where p is an integer and E_n is an energy eigenvalue of the Hamiltonian, $\hat{H}_0$. For small ϵ, the scaled "energies," E_n/g, of the unperturbed system form the real part of the complex decay rates, λ_α. The near degeneracy of the line of eigenvalues in the neighborhood of $\mathrm{Re}(\lambda) = 0$ and $\mathrm{Re}(\lambda) \approx 2$ (for the spectrum in Fig. 1) appears to be due to the splitting of eigenvalues of the outer two wells of the triple well potential due to tunneling between the wells. Since the outer wells are deep and very far apart, the splitting is very small. In order to understand the behavior of the Floquet spectrum, λ_α, at least for small external field amplitude, ϵ, it is useful to look at the classical mechanics underlying this system.

IV. CLASSICAL HAMILTONIAN DYNAMICS

The dynamic evolution of the Brownian particle is largely determined by the "quantum" properties (with g playing the role of Planck's constant) of the system governed by the Hamiltonian, $\hat{H}$, and this in turn is strongly affected by the classical system governed by Hamiltonian, H. Let us therefore examine the dynamics of the classical system governed by the Hamiltonian, H. We first consider the unperturbed system ($\epsilon = 0$).

A. Unperturbed classical system

For the unperturbed classical system, the Hamiltonian can be written

$$H_0 = \frac{p^2}{2} + V_0(x)$$
$$= \frac{p^2}{2} + \frac{g}{2} + \frac{1}{2}(1-3g)x^2 - x^4 + \frac{1}{2}x^6 = E_0, \tag{18}$$

where E_0 is the energy of the classical system and we have made the association, $p = -ig\,\partial/\partial x$ in Eq. (13) (g plays the role of Planck's constant). Hamilton's equations take the form

$$\frac{dp}{dt} = -\frac{\partial H_0}{\partial x} = -(1-3g)x + 4x^3 - 3x^5 \tag{19a}$$

and

$$\frac{dx}{dt} = \frac{\partial H_0}{\partial p} = p. \tag{19b}$$

Fixed points occur when ($dp/dt = 0$, $dx/dt = 0$). The fixed point conditions are satisfied when $(p=0, x=0)$, $(p=0, x = \pm\sqrt{1/3(2+\sqrt{1+9g})})$, and $(p=0, x = \pm\sqrt{1/3(2-\sqrt{1+9g})})$. It is easy to see that for $g < 1/3$, there are five fixed points; three of them are stable and two are unstable. This is due to the fact that the potential, $V_0(x)$, for $g < \frac{1}{3}$ is a triple well system. For $g > 1/3$, there are three fixed points, two are stable and one is unstable. For $g > \frac{1}{3}$, the potential, $V_0(x)$ is a double well potential.

It is important to emphasize that even though the Brownian particle moves in a quartic potential well, the dynamics (for $g < 1/3$) is governed by a Hamiltonian describing a particle in a sixth order polynomial well. For $g < \frac{1}{3}$ the separatrix has an energy given by

$$E_{sx} = \left(\frac{1}{27} - \frac{g}{2}\right) + \left(\frac{1}{27} + \frac{g}{3}\right)\sqrt{1+9g}. \tag{20}$$

For $g > \frac{1}{3}$, the separatrix has energy given by $E_{sx} = g/2$.

The "quantum" version of the unperturbed system (g is Planck's constant) has a ground state energy, $E_0 = 0$, since the stochastic system has a long-time state and therefore must have at least one decay rate, $\mu_0 = E_0/g = 0$. It is possible in principle to transform to action-angle variables. The action is defined

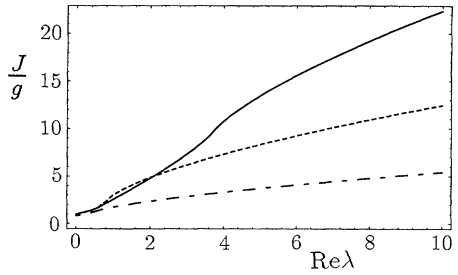

FIG. 2. Plot of J/g versus $\mathrm{Re}(\lambda)=E_0/g$ for (a) $g=0.02$ (solid line), (b) $g=0.1$ (dashed line), (c) $g=1.0$ (dot-dashed line).

$$J=\frac{1}{2\pi}\oint p\,dx=\frac{1}{\pi}\int_{x_L}^{x_R}dx\sqrt{2[E_0-V_o(x)]}. \tag{21}$$

An approximate expression for the allowed energies of the quantum system my be obtained by quantizing the action in units of g. There are a finite number of states between the ground state and the state with the separatrix energy, E_{sx}. Since separatrix energy is a function of g, the number of states in that range is also a function of g. In Fig. 2, we plot J/g versus $\mathrm{Re}\lambda=E_0/g$ for $g=0.02$, 0.1, and 1.0. For $g=0.02$, $g=0.1$, and $g=1.0$ there are approximately 20, 12, and 5 states, respectively, below the value $\mathrm{Re}\lambda=10$. This agrees with observed behavior of the spectrum. Thus, this stochastic system is "quantized" in units of g.

B. Perturbed classical system

For the perturbed classical system, the Hamiltonian is given by

$$H=\frac{p^2}{2}+V_0(x)+\Delta V_\epsilon(x,t), \tag{22}$$

and Hamilton's equations take the form

$$\frac{dp}{dt}=-\frac{\partial H}{\partial x}=-(1-3g)x+4x^3-3x^5-\frac{\partial \Delta V_\epsilon}{\partial x}, \tag{23a}$$

$$\frac{dx}{dt}=\frac{\partial H}{\partial p}=p. \tag{23b}$$

As is well known [1], the time-periodic perturbation induces nonlinear resonances and chaos (chaos results from the overlap of nonlinear resonances) into the classical phase space. Nonlinear resonances occur in regions of phase space where the external field frequency is comensurate with the frequencies, $\omega=\partial E_0/\partial J$, of orbits of the unperturbed system. Since the frequencies of orbits in the neighborhood of a separatrix are small (the frequency of the separatrix itself is zero), when the system is perturbed by an external field with small frequency, chaos only occurs in the neighborhood of the separatrix. External fields with higher frequency can induce nonlinear resonances away from the separatrix and induce global chaos into the system.

In Fig. 3 we show a sequence of strobe plots of the perturbed classical system for diffusion constants $g=0.02$, frequency $\Omega=0.1$, and amplitudes $\epsilon=0.0$, 0.05, and 0.1.

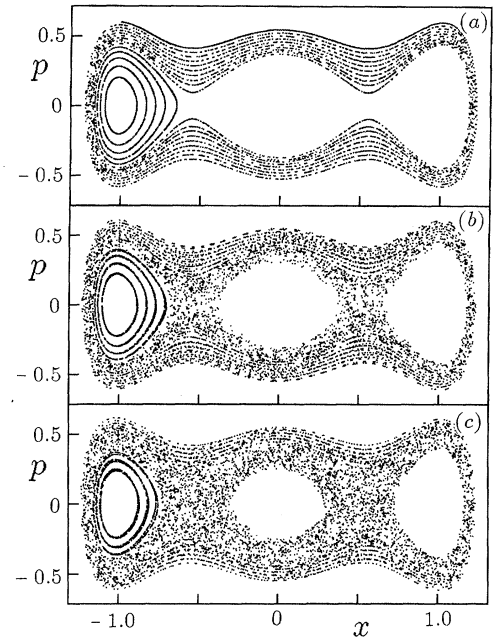

FIG. 3. Strobe plot of the classical phase space for $g=0.02$, $\Omega=0.1$, and (a) $\epsilon=0.0$, (b) $\epsilon=0.05$, and (c) $\epsilon=0.10$.

These correspond to the parameters used for the Floquet spectrum in Fig. 1. For $\epsilon=0$, the region of influence on the Floquet decay rates of the classical separatrix occurs at $\mathrm{Re}(\lambda)=E_{sx}/g\approx 3.73$, where E_{sx} is the separatix energy. Note that there is a qualitative difference in the structure of the Floquet spectrum above and below this value of $\mathrm{Re}(\lambda)$. Let us consider Fig. 3. The trajectories shown are chosen so the initial points have energies, $E_\alpha=g\mathrm{Re}(\lambda_\alpha)$, where values chosen for $\mathrm{Re}(\lambda_\alpha)$ are given by the Floquet rates shown in Fig. 3 (black circles). The innermost curve on the left-hand side has an energy of $E_0=0$. Notice that as the amplitude ϵ increases, the separatrix region in the classical plot becomes chaotic. Note also that the decay rates affected by the chaotic region begin to repell. In Fig. 4, we show a superposition of the Floquet decay rates for amplitudes $\epsilon=0.0$ (the black circles) and $\epsilon=0.05$ (the white circles). The level repulsion can be clearly seen. It is interesting that chaos in the underlying classical system is causing level repulsion in the nearly

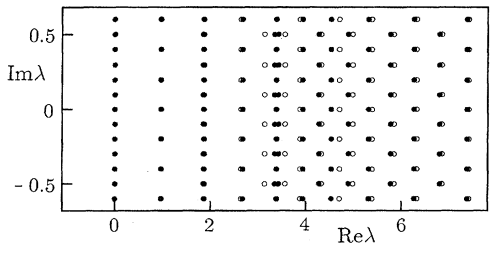

FIG. 4. Partial view of the spectrum of Floquet decay rates for $g=0.02$, $\Omega=0.1$, $\epsilon=0.0$ (black circles), and $\epsilon=0.05$ (white circles). The level repulsion in the region affected by the classical separatrix is clearly seen.

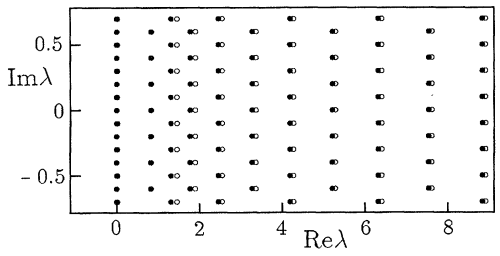

FIG. 5. Partial view of the spectrum of Floquet decay rates for $g=0.1$, $\Omega=0.1$, $\epsilon=0.0$ (black circles), and $\epsilon=0.2$ (white circles).

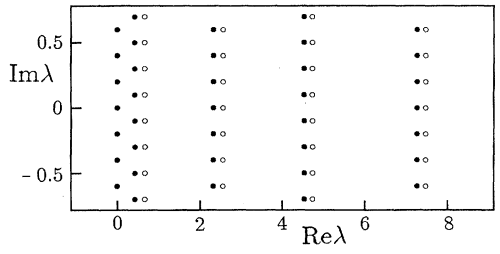

FIG. 7. Partial view of the spectrum of Floquet decay rates for $g=1.0$, $\Omega=0.1$, $\epsilon=0.0$ (black circles), and $\epsilon=1.0$ (white circles).

degenerate eigenstates at $\mathrm{Re}(\lambda)=2$, even though this near degeneracy appears to be due to tunneling between the outer wells. The chaos in the classical phase space is due to a symmetry breaking in the underlying dynamics of the system. This symmetry breaking manifests itself as chaos classically and level repulsion in the stochastic system.

In Fig. 5, we show part of the spectrum of Floquet decay rates for $g=0.1$, $\Omega=0.1$, $\epsilon=0.0$ (black circles), and $\epsilon=0.2$ (white circles). In Fig. 6, we show a sequence of strobe plots for $g=0.1$, $\Omega=0.1$, and amplitudes $\epsilon=0.0$, and $\epsilon=0.2$. The curves are chosen to have initial points with energies, $E_0=g\mathrm{Re}(\lambda)$, where the values of $\mathrm{Re}(\lambda)$ are chosen to coincide with the values shown in Fig. 5 for $\epsilon=0.0$ (black circles). The separatrix in the classical system affects the Floquet spectrum in the neighborhood of $\mathrm{Re}(\lambda)=E_{sx}/g\approx 0.84$. Again, we see level repulsion for those eigenvalues affected by the chaotic region of the classical system.

Finally, in Fig. 7, we show a partial Floquet spectrum for $g=1.0$, $\Omega=0.1$, $\epsilon=0.0$ (black circles) and $\epsilon=1.0$ (white circles). Strobe plots of the classical phase space for $g=1.0$, $\Omega=0.1$, and $\epsilon=0.0$ and 1.0 are shown in Fig. 8. The trajectories are chosen so the initial points have energies $E_0=g\mathrm{Re}(\lambda)$, where the values of $\mathrm{Re}(\lambda)$ are chosen to coincide with the values shown in Fig. 7 for $\epsilon=0$. The Floquet decay rates are affected by the separatrix in the region, $\lambda_{sx}=E_{sx}/g=\frac{1}{2}$. Therefore, the separatrix now lies inside the lowest nonzero decay rate. When chaos occurs in the classical plot, the lowest nonzero decay rate is repelled from the origin. For this case, the onset of chaos will cause a marked increase in the rate of approach of the Brownian particle to its long-time state.

We have found that it is possible to change the rate of approach to the long-time state if chaos in the underlying classical system can affect the neighborhood of the long-time decay rate. Whether or not this can happen depends on the amplitude and frequency of the external field and on the size of the diffusion coefficient, g. Chaos occurs in the region of phase space influenced by nonlinear resonances. These can be moved around in the phase space by changing the frequency, Ω. For very small Ω (what we mean by "small" depends on the system), they only occur in the neighborhood of the separatrix, and therefore, chaos only occurs in the neighborhood of the separatrix. For larger frequencies, Ω, some resonances can be moved away from the separatrix and the chaotic region can be broadened. The diffusion coefficient determines the shape of the potential, $V_0(x)$. However, it also determines the number of states below the separatrix since in the stochastic system the classical action is "quantized" in units of g. Just as for a quantum system, the stochastic system will only be influenced by the chaos if it occupies a region of the classical phase space larger that g

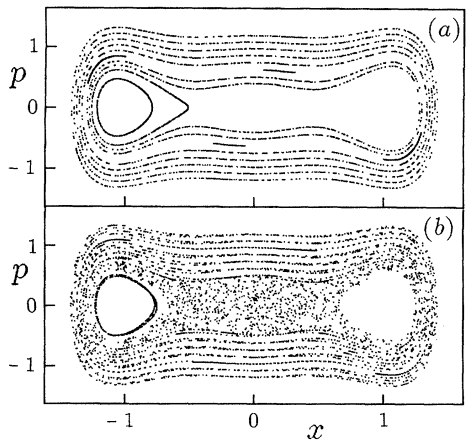

FIG. 6. Strobe plot of the classical phase space for $g=0.1$, $\Omega=0.1$, and (a) $\epsilon=0.0$, (b) $\epsilon=0.2$.

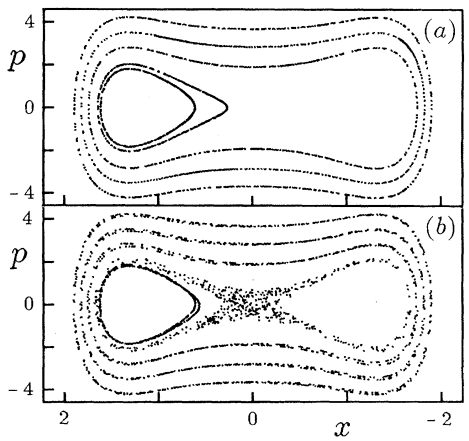

FIG. 8. Strobe plot of the classical phase space for $g=1.0$, $\Omega=0.1$, and (a) $\epsilon=0.0$, (b) $\epsilon=1.0$.

(our effective Planck's constant).

V. STOCHASTIC RESONANCE

In recent years, there has been a great deal of interest in the phenomenon of stochastic resonance. Stochastic resonance can occur in a bistable system when noise is present. If a relatively weak time-periodic external field is applied and if the frequency of the field is of the order of the mean first passage time [17–19] for transitions over the barrier, then the Brownian particle can be entrained by the external field and the response of the system is dramatically enhanced. The Brownian particle will move periodically back and forth across the barrier with a period equal to that of the driving field. Such a phenomenon is of interest because it allows a noisy stochastic system to amplify a weak signal (external driving field). Stochastic resonance is a property of the long-time state of the system. We were interested to see if stochastic resonance had any connection to stochastic chaos, i.e., the transition to chaos in the underlying Hamiltonian system. For the parameter regimes we considered, it did not. For a double well system without a driving field, the long-time decay rate is nearly zero (it is nearly degenerate with the zero eigenvalue). This can be seen in Fig. 1. On the scale of the figure the long-time decay rate is indistinguishable from the eigenvalue with $\mathrm{Re}(\lambda)=0$. They both appear to lie along the same line. Therefore, the mean first passage time is very long and the driving field frequency which resonates with it is very low. The frequency at which stochastic resonance occurs is determined by the first excited state in our unperturbed Hamiltonian system. We can only affect that state if the diffusion coefficient ("Planck's constant") is large enough that the separatrix lies between the ground state and the first excited state.

It is interesting to see how the long-time state changes as we change parameter values. In Fig. 9 we show the long-time state for a fairly small value of the diffusion coefficient, $g=0.1$, and a fairly small value of driving field amplitude, $\epsilon=0.2$, but for a series of decreasing frequencies, $\Omega=1.0$, 0.1, 0.01. We clearly see the system go into a stochastic resonance. In Fig. 10, we show a sequence at higher diffusion coefficient, $g=1.0$, at fixed frequency, $\Omega=0.1$, and increasing field amplitude, $\epsilon=0$, 0.1, 0.5, 1.0. [These results are similar to those in Ref. [6] (1989).] At this higher frequency we can drive the system into stochastic resonance, but it requires a much larger driving field amplitude.

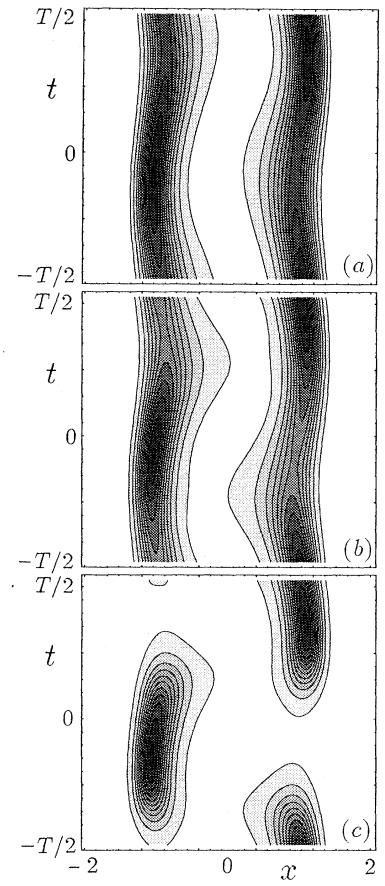

FIG. 9. Sequence of long-time states. The vertical axis is the time ranging over one period of the driving field. The horizontal axis is the spatial coordinate. These plots correspond to $g=0.1$, $\epsilon=0.2$, and (a) $\Omega=1.0$, (b) $\Omega=0.1$, (c) $\Omega=0.01$.

VI. CONCLUSION

There now exist several examples of stochastic systems with detailed balance [2,3,20,21], including the system described here, which show that concepts from "quantum chaos" theory appear to be essential for understanding the stochastic dynamics of Brownian motion with more than one degree of freedom. Such systems may be classified as "integrable" or "nonintegrable" in the same sense that these classifications apply to classical and quantum systems [1]. Analytic solutions of nonintegrable stochastic systems are impossible because such systems are nonseparable. One of the more surprising insights is that the diffusion constant plays a role analogous to Planck's constant in such systems. The stochastic states are actually quantized in units of the diffusion coefficient.

Systems with detailed balance comprise only a fraction of the broad class of stochastic dynamical systems; however, we believe the insights provided by quantum chaos theory for solving these systems may provide a starting point for analyzing systems in which the condition of detailed balance has been relaxed.

ACKNOWLEDGMENTS

The authors wish to thank the Robert A. Welch Foundation, Grant No. F-1051, for support of this work. We also wish to thank The University of Texas System Center for High Performance Computing and the San Diego Super Computer Center for use of their computer facilities.

APPENDIX: FINITE ELEMENT METHOD

We have used the finite element method [22] to solve the eigenvalue problem,

$$\left(\frac{\partial}{\partial t}-\hat{L}_{FP}(x,t)\right)\Phi_\lambda(x,t)=\lambda\Phi_\lambda(x,t) \tag{A1}$$

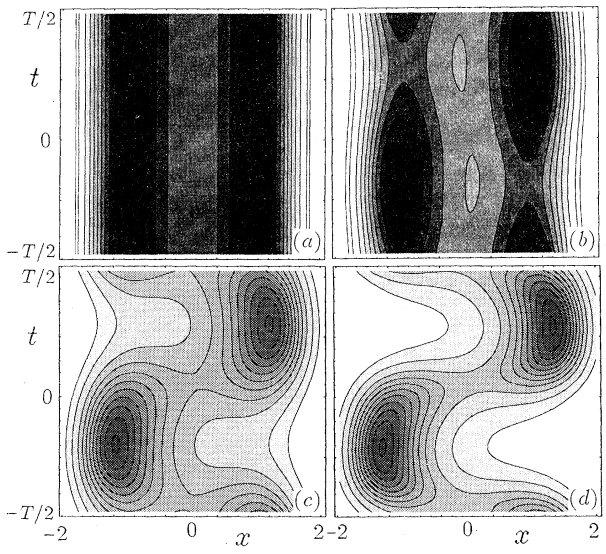

FIG. 10. Sequence of long-time states. The vertical axis is the time ranging over one period of the driving field. The horizontal axis is the spatial coordinate. These plots correspond to $g=1.0$, $\Omega=0.1$, and (a) $\epsilon=0$, (b) $\epsilon=0.1$, (c) $\epsilon=0.5$, (d) $\epsilon=1.0$.

[cf. Eq. (7)] for the Floquet eigenvectors, $\Phi_\lambda(x,t)$, and eigenvalues, λ. We expand $\Phi_\lambda(x,t)$ in terms of finite element basis states, $\phi_i(x)$, in the range $-x_{end}<x<x_{end}$, and in terms of a Fourier time series. We then obtain an approximate expression for the Floquet eigenstate,

$$\Phi_\lambda(x,t)\approx\sum_{i=0}^{N}\sum_{p=-\infty}^{\infty}C_{ip}\phi_i(x)e^{ip\Omega t}. \tag{A2}$$

The finite element basis state, $\phi_i(x)$, is defined as

$$\phi_i(x)=\frac{x-x_i}{x_i-x_{i-1}}\ \text{if}\ x_{i-1}<x<x_i,$$

$$\phi_i(x)=\frac{x_{i+1}-x}{x_{i+1}-x_i}\ \text{if}\ x_i<x<x_{i+1},$$

$$\phi_0(x)=\frac{x_1-x}{x_1-x_0}\ \text{if}\ x_0<x<x_1,$$

$$\phi_N(x)=\frac{x-x_{N-1}}{x_N-x_{N-1}}\ \text{if}\ x_{N-1}<x<x_i, \tag{A3}$$

where $x_0=-x_{end}, x_N=x_{end}$.

Let us now multiply Eq. (A1) by the trial function, $\phi_j(x)$, and integrate over the interval, $x_0\leq x\leq x_N$,

$$\left(-\lambda+\frac{\partial}{\partial t}\right)\int_{x_0}^{x_N}\phi_j(x)\Phi_\lambda(x,t)dx$$

$$=\int_{x_0}^{x_N}\phi_j(x)L_{FP}\Phi_\lambda(x,t)dx,\ \text{with}\ 1\leq j\leq N. \tag{A4}$$

When performing the integration on the right-hand side we can integrate by parts. For example,

$$\int_{x_0}^{x_N}\phi_j(x)\frac{\partial^2}{\partial x^2}\Phi_\lambda(x,t)dx=\phi_j(x)\frac{\partial}{\partial x}\Phi_\lambda(x,t)\Big|_{x_0}^{x_N}-\int_{x_0}^{x_N}\frac{d\phi_j(x)}{dx}\frac{\partial\Phi_\lambda(x,t)}{\partial x}dx. \tag{A5}$$

Here we assume $\Phi_\lambda(\pm x_{end},t)=0$ and $\partial/\partial x\,\Phi_\lambda(\pm x_{end},t)=0$. The end points of the integration must be adjusted until this is true for the eigenstates of interest. Then Eq. (A4) takes the form

$$\sum_i\sum_p(-\lambda+ip\Omega)C_{ip}\int_{-x_{end}}^{x_{end}}\phi_j(x)\phi_i(x)dx=\sum_i\sum_p C_{ip}\int_{-x_{end}}^{x_{end}}\phi_j(x)\frac{d}{dx}[U(x)\phi_i(x)]dx+\sum_i\sum_p\frac{-1}{2i}(C_{i,p-1}-C_{i,p+1})\int_{-x_{end}}^{x_{end}}\phi_j(x)\frac{d\phi_i(x)}{dx}dx-\frac{g}{2}\sum_i\sum_p C_{i,p}\int_{-x_{end}}^{x_{end}}\frac{d\phi_j(x)}{dx}\frac{d\phi_i(x)dx}{dx}, \tag{A6}$$

for $0\leq p\leq\infty$ and $0\leq i\leq N$. The eigenvalue problem can now be solved by the usual matrix solving methods.

[1] L.E. Reichl, *The Transition to Chaos in Conservative Systems: Quantum Manifestations* (Springer-Verlag, New York, 1992).
[2] M. Millonas and L.E. Reichl, Phys. Rev. Lett. **68**, 3125 (1992).
[3] P. Alpatov and L.E. Reichl, Phys. Rev. E **49**, 2630 (1994).
[4] J.B. Swift, P.C. Hohenberg, and G. Ahlers, Phys. Rev. A **43**, 6572 (1991).
[5] P.C. Hohenberg and J.B. Swift, Phys. Rev. A **46**, 4773 (1992).
[6] P. Jung and P. Hanggi, Europhys. Lett. **8**, 505 (1989); Phys. Rev. A **41**, 2977 (1999); **44**, 8032 (1991).
[7] L. Gammaitoni, F. Marchesoni, M. Martinelli, L. Pardi, and S. Santucci, Phys. Lett. A **158**, 449 (1991).
[8] C. Presilla, F. Marchesoni, and L. Gammaitoni, Phys. Rev. A **40**, 2105 (1989).
[9] T. Zhou, F. Moss, and P. Jung, Phys. Rev. A **42**, 3161 (1990).
[10] R. Fox, Phys. Rev. A **39**, 4148 (1989).
[11] B. McNamara and K. Weisenfeld, Phys. Rev. A **39**, 4854 (1989).
[12] R. Benzi, A. Sutera, and A. Vulpiani, J. Phys. A **14**, L453 (1981).
[13] C. Nicolis and G. Nicolis, Tellus **33**, 225 (1981).
[14] M.I. Dykman, R. Mannella, P.V.E. McClintock, and N.G. Stock, Phys. Rev. Lett. **68**, 2985 (1992).

[15] M.I. Dykman, M.M. Millonas, and V.N. Smelyanskiy, Phys. Lett. A **195**, 53 (1994).
[16] H. Risken, *The Fokker-Planck Equation* (Springer-Verlag, Berlin, 1984).
[17] C.W. Gardiner, *Handbook of Stochastic Methods* (Springer-Verlag, Berlin, 1985).
[18] N.G. van Kampen, J. Stat. Phys. **17**, 71 (1977).
[19] L.E. Reichl, J. Chem. Phys. **77**, 4199 (1982).
[20] P. Alpatov and L.E. Reichl, Phys. Rev. E **52**, 4516 (1995).
[21] R. Graham and T. Tel, Phys. Rev. lett. **52**, 9 (1984).
[22] M. Mori, *The Finite Element Method and Its Applications* (MacMillan, London, 1983).

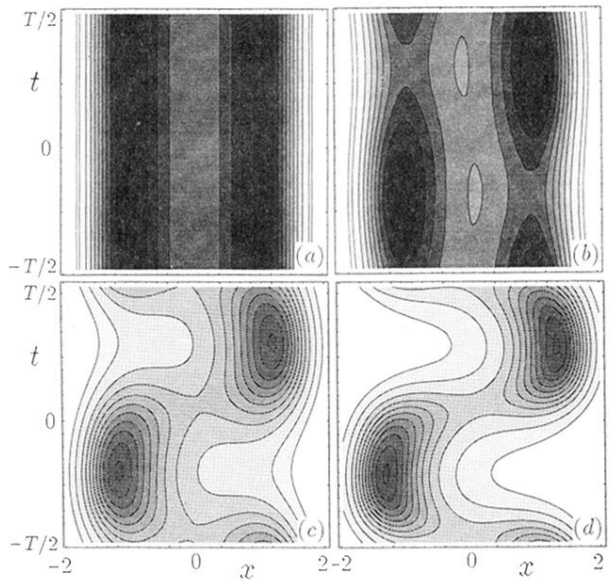

FIG. 10. Sequence of long-time states. The vertical axis is the time ranging over one period of the driving field. The horizontal axis is the spatial coordinate. These plots correspond to $g=1.0$, $\Omega=0.1$, and (a) $\epsilon=0$, (b) $\epsilon=0.1$, (c) $\epsilon=0.5$, (d) $\epsilon=1.0$.